Sains Malaysiana 54(7)(2025): 1813-1821
http://doi.org/10.17576/jsm-2025-5407-14

Resin-Mxene Composite for Electromagnetic Shielding Applications

(Komposit Resin-Mxene untuk Aplikasi Perisai Elektromagnet)

AZKA REHMAN[1], NUR AZREEN AZHAR[1], HUDA A MAJID[2], HERDAWATIE ABDUL KADIR[3] & FAHMIRUDDIN ESA[1,*]

[1]Department of Physics and Chemistry, Faculty of Applied Sciences and Technology,Universiti Tun Hussein Onn Malaysia, Pagoh Higher Education Hub, KM 1, Jalan Panchor, 84600 Panchor, Johor, Malaysia
[2]Department of Electrical Engineering Technology, Faculty of Engineering Technology, Universiti Tun Hussein Onn Malaysia, Pagoh Higher Education Hub, KM 1, Jalan Panchor, 84600 Panchor, Johor, Malaysia
[3]Department of Electronic Engineering, Faculty of Engineering, Universiti Tun Hussein Onn Malaysia, 86400 Parit Raja, Johor, Malaysia

Received: 17 February 2025/Accepted: 16 May 2025

ABSTRACT

The growing demand for advanced electromagnetic interference (EMI) shielding materials has driven the development of lightweight high-performance solutions for modern electronics. In this study, $Mo_2Ti_2C_3$ MXene was synthesized via selective etching of the $Mo_2Ti_2AlC_3$ MAX phase using hydrofluoric acid (HF) at concentrations of 6M and 9M. The synthesized MXene was then incorporated into a resin matrix to fabricate MXene-based composites with varying filler loadings of 1 wt.%, 3 wt.%, and 5 wt.% for EMI shielding applications. Fourier-transform infrared spectroscopy (FTIR) confirmed that 9M HF etching resulted in higher surface functionalization, with pronounced –OH, –O, and –F terminations, which enhanced electrical conductivity. Field-emission scanning electron microscopy (FESEM) showed a morphological transition from a compact MAX phase to a characteristic stacked lamellar MXene structure, while energy-dispersive X-ray spectroscopy (EDX) validated the complete removal of aluminum. X-ray diffraction (XRD) analysis demonstrated that the incorporation of 3 wt.% MXene into the resin matrix yielded the highest crystallinity, suggesting strong interfacial interactions. Reflection coefficient (S11) measurements in the X-band (8.2–12.4 GHz) showed that a higher MXene content enhanced wave reflection, improving EMI shielding. The 3 wt.% MXene composite achieved optimal performance by balancing reflection and absorption, minimizing transmitted interference. These findings demonstrate that the 9M HF-etched $Mo_2Ti_2C_3$ MXene with 3 wt.% filler loading provides the best balance of electrical conductivity, structural stability, and EMI shielding effectiveness, making it a promising candidate for next-generation electronic and communication applications.

Keywords: EMI shielding; HF etching; $Mo_2Ti_2C_3$ MXene; reflection coefficient

ABSTRAK

Permintaan yang semakin meningkat untuk bahan perisai gangguan elektromagnet termaju (EMI) telah mendorong pembangunan penyelesaian berprestasi tinggi ringan untuk elektronik moden. Dalam kajian ini, $Mo_2Ti_2C_3$ MXene telah disintesis melalui punaran terpilih fasa MAX $Mo_2Ti_2AlC_3$ menggunakan asid hidrofluorik (HF) pada kepekatan 6M dan 9M. MXene yang disintesis kemudiannya digabungkan ke dalam matriks resin untuk menghasilkan komposit berasaskan MXene dengan beban pengisi yang berbeza-beza 1 %bt., 3 %bt. dan 5 %bt. untuk aplikasi pelindung EMI. Spektroskopi inframerah transformasi Fourier (FTIR) mengesahkan bahawa punaran HF 9M menghasilkan kefungsian permukaan yang lebih tinggi dengan penamatan –OH, –O dan –F yang disebut, yang meningkatkan kekonduksian elektrik. Mikroskopi elektron pengimbasan pelepasan medan (FESEM) mendedahkan peralihan morfologi daripada fasa MAX padat kepada struktur bertindan ciri MXene lamelar, manakala spektroskopi sinar-X (EDX) penyebaran tenaga mengesahkan penyingkiran lengkap aluminium. Analisis pembelauan sinar-X (XRD) menunjukkan bahawa penggabungan 3 wt.% MXene ke dalam matriks resin menghasilkan kehabluran tertinggi, mencadangkan interaksi antara muka yang kuat. Pengukuran pekali pantulan (S11) dalam jalur X (8.2-12.4 GHz) menunjukkan bahawa kandungan MXene yang lebih tinggi meningkatkan pantulan gelombang, meningkatkan perisai EMI. Komposit MXene 3 wt.% mencapai prestasi optimum dengan mengimbangi pantulan dan penyerapan, meminimumkan gangguan yang dihantar. Penemuan ini menunjukkan bahawa MXene $Mo_2Ti_2C_3$ MXene 9M HF dengan pemuatan pengisi 3 wt.% memberikan keseimbangan terbaik kekonduksian elektrik, kestabilan struktur dan keberkesanan perisai EMI, menjadikannya calon yang berpotensi untuk aplikasi elektronik dan komunikasi generasi akan datang.

Kata kunci: $Mo_2Ti_2C_3$ MXene; pekali pantulan; perisai EMI; punaran HF

INTRODUCTION

The rapid expansion of wireless communication systems and high-frequency electronic devices has intensified the need for effective electromagnetic interference (EMI) shielding materials (Choi et al. 2022; Nguyen & Choi 2024). EMI can degrade signal integrity, disrupt electronic circuits, and pose safety risks in critical sectors, such as aerospace, defense, healthcare, and telecommunications (James & Choi 2024; Umadevi & Ranganathan 2024). Conventional shielding materials, including metals and carbon-based composites, provide effective shielding, but suffer from drawbacks such as high density, corrosion susceptibility, and limited mechanical flexibility (Opara et al. 2023; Yang et al. 2024). These limitations necessitate the development of lightweight, corrosion-resistant, and high-performance EMI shielding materials for modern electronic applications (Karahan et al. 2025).

Two-dimensional (2D) materials such as graphene, transition metal dichalcogenides (TMDs), boron nitride (BN), and MXenes have emerged as highly promising candidates for EMI shielding because of their exceptional electrical conductivity, large surface area, and tunable physicochemical properties (Kumari et al. 2023; Raagulan, Kim & Chai 2020; Zhang et al. 2021). Among these, MXenes, a class of transition metal carbides, nitrides, and carbonitrides, have garnered significant attention owing to their unique metallic conductivities, layered architectures, and excellent processabilities (Kim & Byun 2024). The general formula of MXenes is $M_{n+1}X_nT_x$, where M represents a transition metal, X denotes carbon and/or nitrogen, and T_x refers to surface terminations such as –OH, –O, and –F (Iqbal et al. 2021). $Mo_2Ti_2C_3$ MXene, a double-transition metal MXene, exhibits remarkable electrical and mechanical properties, making it a strong candidate for shielding applications (Liu et al. 2023). However, its practical implementation is hindered by its structural instability, oxidation susceptibility, and mechanical fragility (Khalid et al. 2025). Additionally, the synthesis of MXene from the MAX phase using hydrofluoric acid (HF) etching presents challenges; excessive HF etching compromises the structural integrity, whereas insufficient etching leaves residual impurities that degrade the electrical performance (Wong, Lim & Seh 2022).

To address these limitations, the incorporation of MXenes into polymeric matrices, such as resins, offers a promising approach to enhance mechanical strength, stability, and processability while retaining superior shielding properties (Ghamsarizade, Ramezanzadeh & Mohammadloo 2023; Gong et al. 2021). This hybrid composite approach is expected to provide lightweight, flexible, and high-performance materials for EMI shielding applications. However, further research is required to optimize the MXene-polymer interactions, refine the composite microstructure, and assess its shielding effectiveness across different frequency ranges.

To gain a comprehensive understanding of its structural, chemical, and shielding properties, the composite was analyzed using various characterization techniques. Fourier-transform infrared spectroscopy (FTIR) was used to identify the functional groups, while X-ray diffraction (XRD) provided insights into the crystallographic structure. Field-emission scanning electron microscopy (FESEM) was used to examine the morphology of the material and energy-dispersive X-ray spectroscopy (EDX) was used to determine the elemental composition. Moreover, reflection coefficient (S11) measurements were performed to assess the electromagnetic response. The insights gained from this study will contribute to the advancement of MXene-based composites and pave the way for scalable high-performance EMI shielding materials for next-generation electronics and communication technologies.

METHODOLOGY

PREPARATION OF MXENES VIA CHEMICAL ETCHING

$Mo_2Ti_2C_3$ MXene was synthesized via a chemical etching process (Mendes et al. 2020). The precursor material used was molybdenum titanium aluminum carbide ($Mo_2Ti_2AlC_3$) powder, purchased from Sigma-Aldrich. The etching solution was prepared by dissolving 0.6667 g of lithium fluoride (LiF) into a mixture of 44.70 mL concentrated hydrochloric acid (37%) and 15.30 mL deionized water. The solution was stirred continuously at 24 °C for 30 min in a chemical fume hood to ensure homogeneity. After the complete dissolution of LiF, 1 g of $Mo_2Ti_2AlC_3$ powder was gradually added to the etching solution. The reaction mixture was maintained at 35 °C under continuous magnetic stirring at 500 rpm for 96 h to enable selective removal of aluminum layers from the MAX phase.

Upon completion of the etching process, the resulting suspension was subjected to successive washing and centrifugation cycles (3000 rpm, 20 min, 24 °C). These cycles were repeated until the pH of the supernatant reached a neutral value between 6 and 7, indicating the effective removal of residual acids. The final $Mo_2Ti_2C_3$ MXene sediment was placed in an oven and dried at 110 °C for a duration of 24 h.

FUNCTIONAL GROUP, MORPHOLOGICAL AND ELEMENTAL TRACING

The dried MXene powder was analyzed to confirm its structural, chemical, and morphological properties. Surface functional groups were identified using Fourier Transform Infrared Spectroscopy (FTIR) on a Spectrum Two FT-IR Spectrometer (PerkinElmer, USA). Morphology and elemental composition were examined using Field Emission Scanning Electron Microscopy (FESEM) combined with Energy Dispersive X-ray Spectroscopy (EDX) on an FEI Versa 3D Dual Beam system (Thermo Fisher Scientific, USA).

RESIN-MXENE COMPOSITE PREPARATION

Dried MXene powder was added to UV-curable photopolymer resin at specific weight percentages of 1%, 3%, and 5%. The blends were first stirred mechanically for 30 min to facilitate initial dispersion, then ultrasonicated at 40 kHz for 15 min to achieve homogeneity in the MXene dispersion within the resin matrix.

Each formulation was subsequently loaded into the resin tank of a Elegoo Mars 5 Ultra 3D printer, as shown in Figure 1. The samples were printed in X-band rectangular dimensions (22.86 × 10.16 mm) with a thickness of 4 mm through a layer-by-layer photopolymerization process comprising approximately 230 layers over a 50-min printing duration.

Upon completion of the printing process, the composite samples were rinsed thoroughly with isopropyl alcohol (IPA) to remove any uncured resin. They were then dried and post-cured using Anycubic Wash and Cure Station under 365 nm UV light exposure. The final cured samples were precisely fitted into an X-band waveguide assembly with a metallic backing plate for subsequent electromagnetic characterization.

STRUCTURAL AND REFLECTION COEFFICIENT CHARACTERISTICS

The electromagnetic properties of the cured rectangular composites were assessed by measuring the reflection coefficient (S_{11}) across the X-band frequency range (8.2-12.4 GHz). These measurements were conducted using an N5234B PNA-L Microwave Network Analyzer (Keysight Technologies, USA) with a one-port reflection setup. Moreover, the structural characteristics of the thin film composites were assessed using X-ray Diffraction (XRD) with an X'Pert³ Powder Diffractometer (Malvern Panalytical, Netherlands), equipped with a thin film module and Cu-Kα radiation, to detect changes in crystallinity and interlayer spacing resulting from MXene incorporation into the polymer matrix.

RESULTS AND DISCUSSION

Figure 2 showed the FTIR spectra of $Mo_2Ti_2AlC_3$ MAX phase into its MXene derivatives, which were etched with 6M and 9M HF solutions. The FTIR spectrum of the MAX phase shows no significant peaks, indicating that it maintains its structural purity (Haq et al. 2022). In contrast, the MXene spectra display distinct, low-intensity peaks, which suggest that surface terminations and molecular vibrations were introduced during the etching process. Significantly, the 9M etched MXene shows more pronounced low-intensity peaks than the 6M, indicating a higher level of etching and surface functionalization (Ahmaruzzaman 2022). The peaks at 2329, 2133, and 1999 cm^{-1} correspond to stretching vibrations of C=O, C≡C, and C=C, respectively. The peaks at 560 cm^{-1} and 668 cm^{-1} are attributed to the deformation vibrations of Mo–O and Ti–O bonds, highlighting structural changes (Ali, Haider & Rizwan 2022). Additionally, the peaks at 3419 cm^{-1} and 1645 cm^{-1} indicate O–H stretching and bending vibrations, pointing to the presence of oxygen-containing functional groups (Bibi et al. 2024). A weak band at 1203 cm^{-1} suggests C–F groups, likely introduced due to the HF etching process. Moreover, the peaks at 1704 cm^{-1} (C=O) and 2912 cm^{-1} (C–H stretching) point to residual carbonaceous groups (Parker et al. 2024). A broad band in the range of 3560 to 3900 cm^{-1} indicates O-H stretching vibrations, likely due to moisture or background effects (Ikemoto et al. 2022). However, the 9M HF etching achieved more extensive surface functionalization than the 6M, with higher

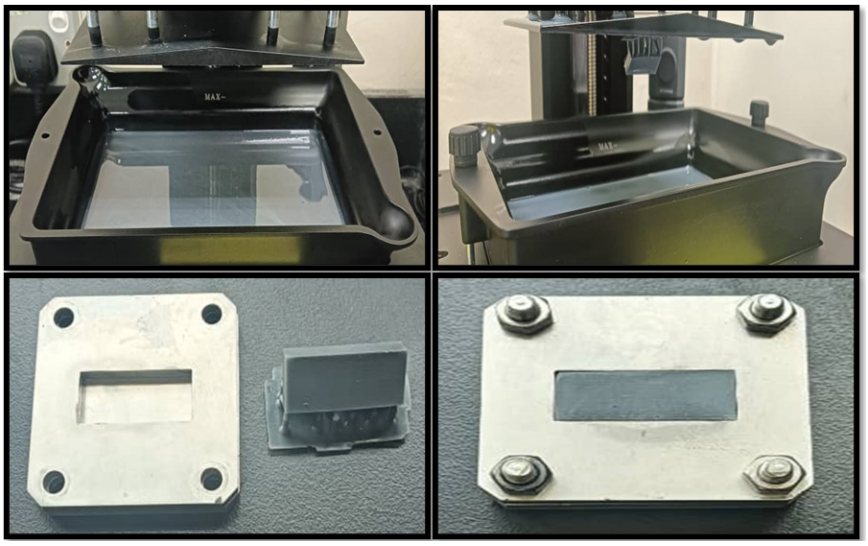

FIGURE 1. Preparation of MXene/resin composites via 3D printing, followed by UV curing and assembly for microwave measurement

intensity peaks corresponding to –O, –OH, and –F surface terminations. This enhanced functionalization makes the 9M etched MXene ideal for advanced characterization and applications in electromagnetic shielding.

Figure 3 presents the FESEM analysis of both the $Mo_2Ti_2AlC_3$ MAX phase and $Mo_2Ti_2C_3$ MXene derivatives. The FESEM analysis of the $Mo_2Ti_2AlC_3$ MAX phase (Figure 2(a)) shows a compact and irregular morphology, with a densely packed structure (Babar et al. 2020). This compactness reflects the strong and robust nature of the material before etching. In contrast, $Mo_2Ti_2C_3$ MXene (Figure 2(b)), which was etched with 9M HF, displays a distinct, stacked lamellar morphology (Bibi et al. 2024). This change in structure was due to the selective removal of the aluminum (Al) layer during the etching process. The resulting layered structure is held together by strong van der Waals interactions between the MXene layers, which aligns with the expected morphology of the 2D materials (Nasrin et al. 2022).

Table 1 shows the EDX analysis of both the $Mo_2Ti_2AlC_3$ MAX phase and the 9M etched $Mo_2Ti_2C_3$ MXene. The EDX spectrum of the $Mo_2Ti_2AlC_3$ MAX phase confirmed the presence of Mo, Ti, Al, and C, indicating that the MAX phase was successfully synthesized. After HF etching, the EDX analysis of the resulting 9M $Mo_2Ti_2C_3$ MXene shows the absence of aluminium (Al), confirming that the Al layer was effectively removed during the etching process. Moreover, the presence of surface terminations such as –OH, –F, and –O, which are characteristic of the etching process, plays a crucial role in EMI shielding applications (Iqbal et al. 2021; Verma et al. 2022). These functional groups enhance surface activity, facilitate charge transport, and contribute to polarization loss and dielectric dissipation, thereby improving electromagnetic wave attenuation and overall shielding effectiveness (Habibpour et al. 2022; Ulas et al. 2024).

Figure 4 presents the XRD patterns of pure resin and its composites containing $Mo_2Ti_2C_3$ MXene. The MXene was synthesized using 9 M hydrofluoric acid (HF) and incorporated into the resin at various concentrations of 1 wt.%, 3 wt.%, and 5 wt.%. The pure resin exhibits a broad amorphous peak at **19.72° (002)** (Park, Lee & Kim 2024), which decreases in intensity as MXene is added, indicating a reduction in amorphous content due to **two factors**: (1) the crystalline MXene phase diluting the resin matrix (Li et al. 2022), and (2) interfacial interactions restricting polymer chain mobility (Tu et al. 2024). Distinct MXene peaks appear at **14.90° (004), 22.60° (006), and 30.19° (008)**, confirming its layered structure (De Jesús Báez et al. 2023; Gandla, Zhang & Tan 2022; Li et al. 2015), while additional peaks (**34°-41.51°**) correspond to titanium and molybdenum carbide phases (Feng et al. 2019; Gandla, Zhang & Tan 2022).

Moreover, the concentration-dependent behavior shows three distinct regimes; at **1 wt.%**, MXene peaks are absent, likely due to exfoliation below detection limits (Carey et al. 2019); the **3 wt.%** composite shows sharp, well-defined peaks, suggesting optimal dispersion (Munir et al. 2020; Tanvir et al. 2019), indicating excellent dispersion approaching the percolation threshold; while **5 wt.%** exhibits peak broadening, indicating aggregation or defects (Lipatov et al. 2016; Ramesh et al. 2022).

The structural evolution shows a semi-crystalline composite, where MXene's crystalline domains progressively disrupt the resin's amorphous structure (Chetana et al. 2023; Hu et al. 2022). This transition, combined with the presence of secondary carbide phases, enhances the composite's functional properties, making it suitable for advanced applications (Han et al. 2023), making it suitable for advanced applications (Ling et al. 2024).

Figure 5 illustrates the reflection coefficient (S11) behavior of $Mo_2Ti_2C_3$ MXene-based composites across the X-band frequency range (8.2-12.4 GHz), demonstrating their electromagnetic interference (EMI) shielding potential. The results show a clear trend: as the MXene content increases, the reflection coefficient rises, indicating enhanced reflectivity and shielding effectiveness. This increase can be attributed to the intrinsic high electrical conductivity and permittivity of MXene, which impede the penetration of incident electromagnetic waves, thereby promoting reflection (Jia et al. 2020). As a conductive filler, MXene creates an interconnected network within the resin matrix, improving charge transport and enabling the formation of localized electric fields that enhance surface reflection (Han et al. 2015). The rise in reflection coefficient with filler content is consistent with classical shielding theory, where materials with high conductivity reflect more incident energy due to the skin effect and impedance mismatch with air (Peng & Qin 2021).

Moreover, the random distribution of MXene flakes within the polymer matrix likely induces multiple internal reflections, further increasing the reflection coefficient. These internal reflections are especially significant in heterogeneous composites, where conductive fillers are dispersed throughout a low-permittivity host material. As microwaves interact with these interfaces, they experience successive reflections and scattering, resulting in reduced transmission (Islam et al. 2023).

The resin in this system functions primarily as a structural support and dispersive medium, contributing minimal electromagnetic properties on its own. However, it offers the advantages of low cost, processability, and mechanical stability, making it an effective matrix for EMI shielding composites. A comparison with other two-dimensional conductive fillers, such as graphene, shows similar reflection-dominant behaviour. Graphene-based composites also exhibit increased reflection coefficients with higher filler loadings due to their superior electrical conductivity and layered structure (Osman et al. 2022). However, MXenes offer advantages such as tunable surface terminations, improved wettability,

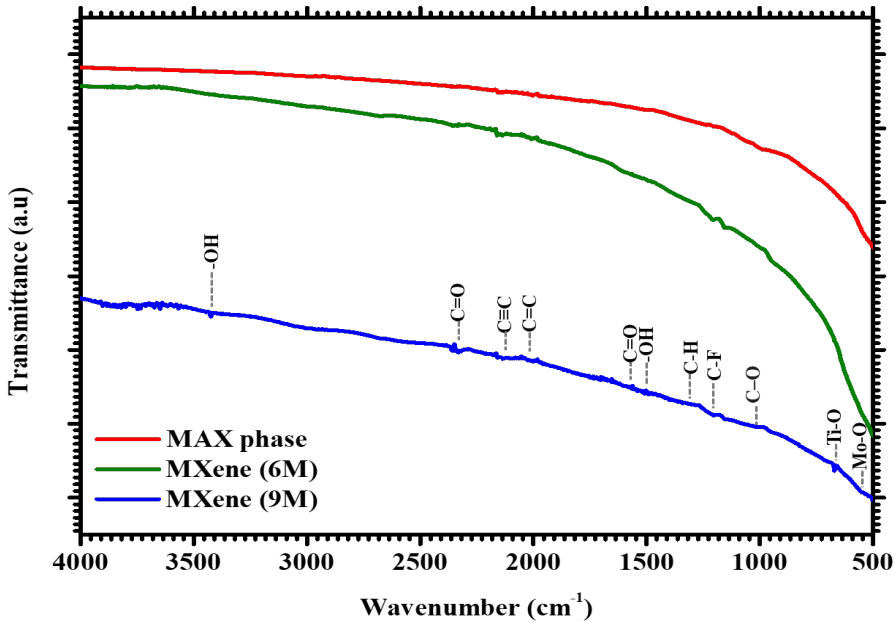

FIGURE 2. FTIR spectra of MAX phase and Mxene derivatives

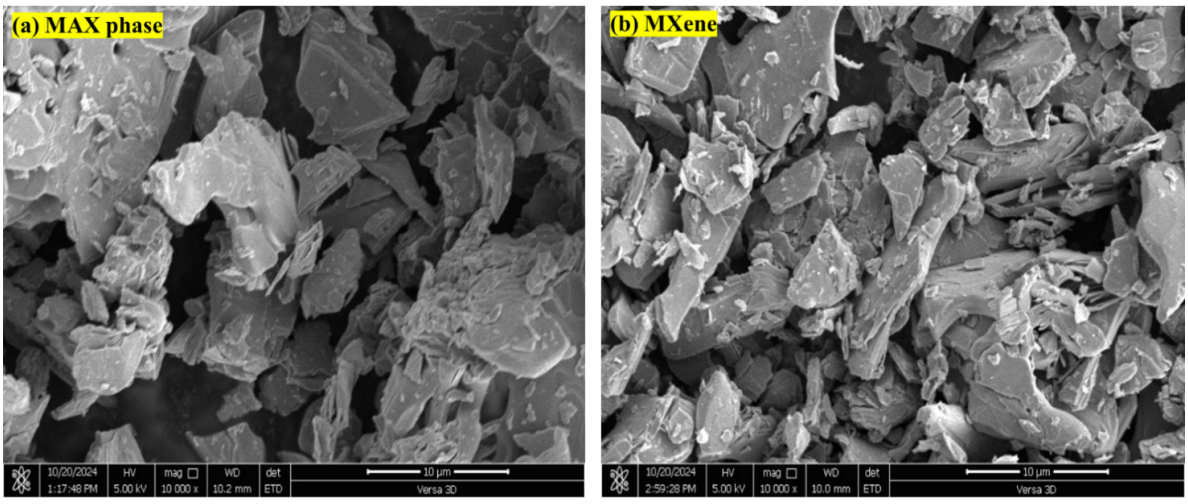

FIGURE 3. Morphology of (a) MAX phase and (b) 9M etched MXene in powder form

TABLE 1. Elemental compositional analysis of MAX phase and 9M etched MXene

Element	MAX phase		9M etched MXene	
	Weight %	Atomic %	Weight %	Atomic %
Mo	222.25 ± 39.69	14.27	184.44 ± 35.41	9.75
Al	23.41 ± 4.15	5.34		
Ti	69.01 ± 180.68	8.87	102.18 ± 146.33	10.82
C	122.40 ± 10.91	62.76	129.70 ± 9.57	54.78
O	22.73 ± 5.29	8.75	77.73 ± 7.32	24.65
Total	459.80	100	494.04	100

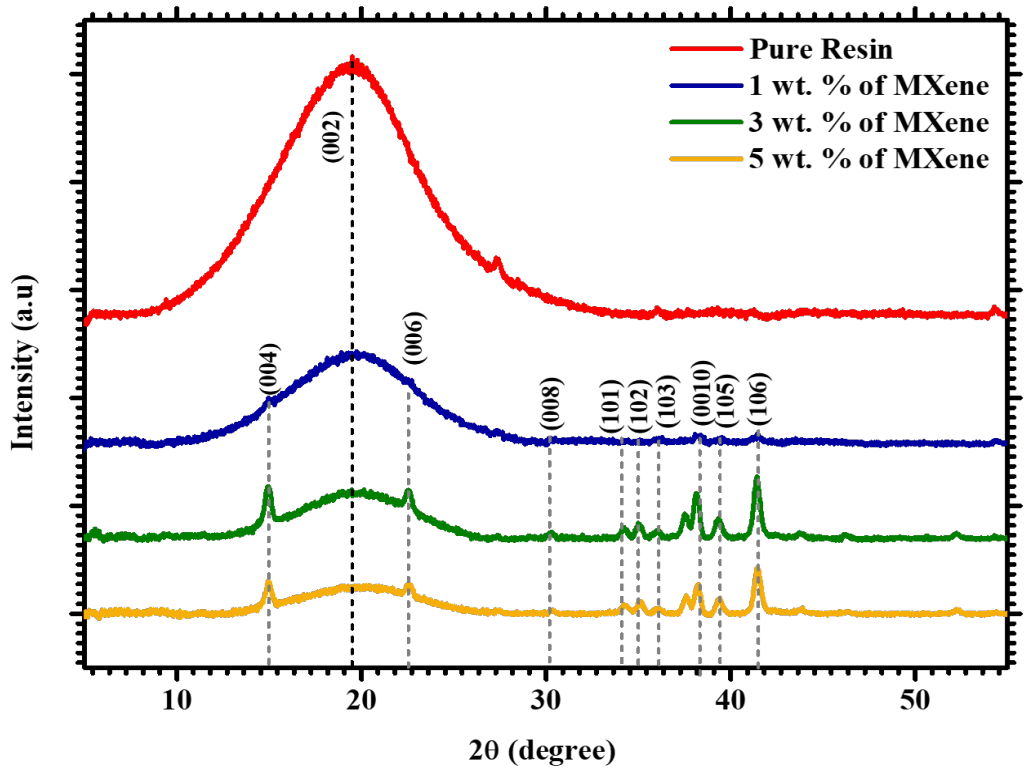

FIGURE 4. XRD patterns of pure resin and its composites with varying MXene ($Mo_2Ti_2C_3$) content (1 wt.%, 3 wt.%, and 5 wt.%)

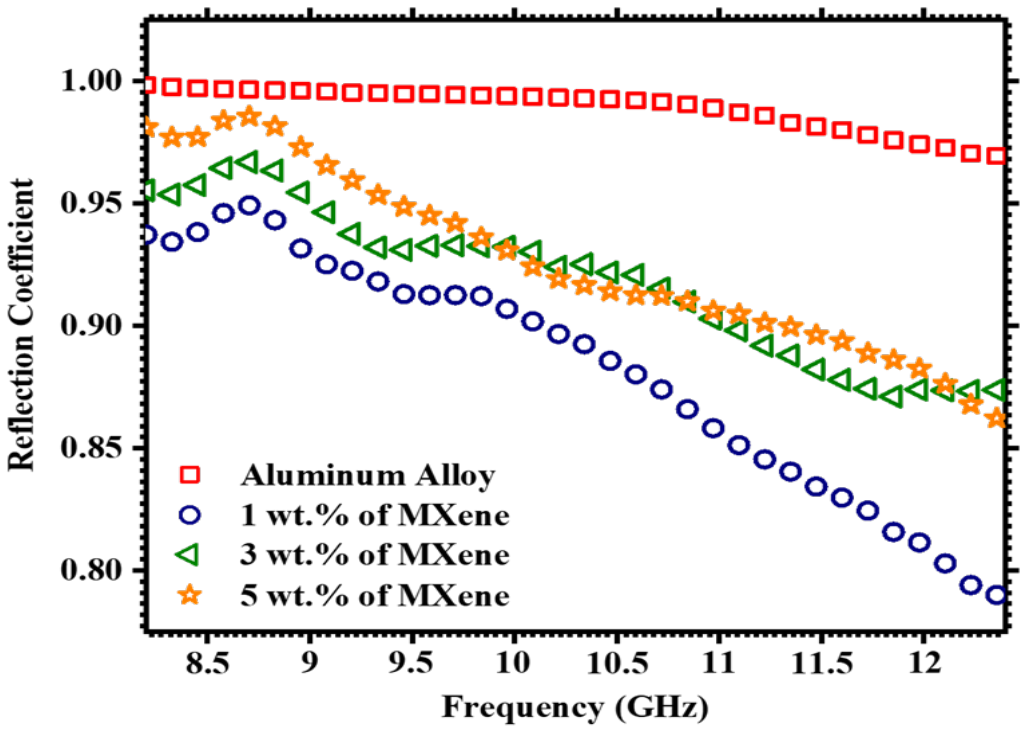

FIGURE 5. Reflection coefficient (S11) versus frequency of MXene-based materials at varying concentrations

and higher dielectric loss, making them more effective in certain microwave applications (Zhang et al. 2023). Among the studied formulations, the composite with 3 wt.% MXene exhibited the most balanced shielding performance. It achieved high reflection without compromising absorption, likely due to optimal filler dispersion and interfacial polarization. Excessive MXene loading (5 wt.%) may lead to aggregation, which disrupts uniform conductivity pathways and increases impedance mismatches, slightly diminishing overall performance.

These findings underscore the suitability of $Mo_2Ti_2C_3$ MXene composites for advanced EMI shielding applications. Their reflection-dominant behavior, coupled with adjustable dielectric properties and excellent processability, positions them as strong candidates for use in aerospace, electronics, and communication systems (Chand, Zhang & Chen 2022; Protyai & Rashid 2024).

CONCLUSIONS

This study demonstrated the successful synthesis and characterization of $Mo_2Ti_2C_3$ MXene and its resin-based composites for EMI shielding applications. FTIR analysis confirmed the effective etching of the MAX phase using 6M and 9M HF, with the 9M etched MXene exhibiting more pronounced surface functionalization due to enhanced –O, –OH, and –F terminations. FESEM showed the transformation of the compact MAX phase into a stacked lamellar MXene structure, while EDX confirmed the complete removal of Al, validating the selective etching process. XRD analysis demonstrated that the incorporation of 3 wt.% MXene into the resin matrix yielded the highest crystallinity, suggesting strong interfacial interactions. Reflection coefficient (S11) measurements in the X-band (8.2-12.4 GHz) showed that a higher MXene content enhanced wave reflection, improving EMI shielding. The 3 wt.% MXene composite achieved optimal performance by balancing reflection and absorption, minimizing transmitted interference. These findings demonstrate that 9M HF-etched $Mo_2Ti_2C_3$ MXene at 3 wt.% loading in resin provides the best balance of electrical conductivity, structural stability, and EMI shielding effectiveness, making it a promising candidate for next-generation electronic and communication applications.

ACKNOWLEDGEMENTS

This research was supported by Universiti Tun Hussein Onn Malaysia through the Multidisciplinary Research Grant (MDR), Q692. Sincere thanks to Mohammad Khairul Nahar Kassim and Muhammad Amiruddin Hassan Al Ashari from the UTHM Laboratory Management Office - Pagoh Branch Campus for their invaluable assistance with the sample characterizations.

REFERENCES

Ahmaruzzaman, M. 2022. MXenes and MXene-supported nanocomposites: A novel materials for aqueous environmental remediation. *RSC Advances* 12(53): 34766-34789.

Ali, I., Haider, Z. & Rizwan, S. 2022. Enhanced pseudocapacitive energy storage and thermal stability of Sn 2^+ ion-intercalated molybdenum titanium carbide (Mo_2TiC_2) MXene. *RSC Advances* 12(49): 31923-31934.

Babar, Z.U.D., Fatheema, J., Arif, N., Anwar, M.S., Gul, S., Iqbal, M. & Rizwan, S. 2020. Magnetic phase transition from paramagnetic in Nb_2 AlC-MAX to superconductivity-like diamagnetic in Nb_2C-MXene: An experimental and computational analysis. *RSC Advances* 10(43): 25669-25678.

Bibi, F., Numan, A., Tan, Y.S. & Mohammad, K. 2024. Facile extraction of $Mo_2Ti_2C_3Tx$ MXene via hydrothermal synthesis for electrochemical energy storage. *Journal of Energy Storage* 85: 111154.

Carey, M.S., Sokol, M., Palmese, G.R. & Barsoum, M.W. 2019. Water transport and thermomechanical properties of $Ti_3C_2T_z$ MXene epoxy nanocomposites. *ACS Applied Materials & Interfaces* 11(42): 39143-39149.

Chand, K., Zhang, X. & Chen, Y. 2022. Recent progress in MXene and graphene based nanocomposites for microwave absorption and electromagnetic interference shielding. *Arabian Journal of Chemistry* 15(10): 104143.

Chetana, S., Muhammad Amirul Aizat Mohd Abdah, Thakur, V.N., Govinde Gowda, M.S., Choudhary, P., Sriramoju, J.B., Rangappa, D., Malik, S., Rustagi, S. & Khalid, M. 2023. Progress and prospects of MXene-based hybrid composites for next-generation energy technology. *Journal of the Electrochemical Society* 170(12): 120530.

Choi, H.K., Lee, D.S., Bae, S., Moon, B.J., Lee, S-K. & Kim, T-W. 2022. Recent progress of research into conductive nanomaterials for use in electromagnetic interference shields. *Applied Science and Convergence Technology* 31(6): 120-127.

De Jesús Báez, L.R., Rosas, A.S., Mahale, P. & Mallouk, T.E. 2023. Chelation-based route to aluminum-free layered transition metal carbides (MXenes). *ACS Omega* 8(44): 41969-41976.

Feng, W., Luo, H., Wang, Y., Zeng, S., Tan, Y., Deng, L., Zhou, X., Zhang, H. & Peng, S. 2019. Mxenes derived laminated and magnetic composites with excellent microwave absorbing performance. *Scientific Reports* 9: 3957.

Gandla, D., Zhang, F. & Tan, D.Q. 2022. Advantage of larger interlayer spacing of a $Mo_2Ti_2C_3$ MXene free-standing film electrode toward an excellent performance supercapacitor in a binary ionic liquid–organic electrolyte. *ACS Omega* 7(8): 7190-7198.

Ghamsarizade, R., Ramezanzadeh, B. & Mohammadloo, H.E. 2023. A review on recent advances in 2D-transition metal carbonitride-MXenes nano-sheets/polymer composites' electromagnetic shields, mechanical and thermal properties. *Journal of the Taiwan Institute of Chemical Engineers* 144: 104740.

Gong, K., Zhou, K., Qian, X., Shi, C. & Yu, B. 2021. MXene as emerging nanofillers for high-performance polymer composites: A review. *Composites Part B: Engineering* 217: 108867.

Habibpour, S., Zarshenas, K., Zhang, M., Hamidinejad, M., Ma, L., Park, C.B. & Yu, A. 2022. Greatly enhanced electromagnetic interference shielding effectiveness and mechanical properties of polyaniline-grafted $Ti_3C_2T_x$ MXene–PVDF composites. *ACS Applied Materials & Interfaces* 14(18): 21521-21534.

Han, R., Li, W., Zhu, M. & Li, F. 2015. An enhancement of reflection loss by controlling the reflected electromagnetic wave at air–absorber interface. *Applied Physics A* 119: 201-204.

Han, X., Qiu, X., Zong, M. & Hao, J. 2023. Assembled MXene macrostructures for multifunctional polymer nanocomposites. *Small Structures* 4(10): 2300090.

Haq, Y-U., Ullah, R., Mazhar, S., Khattak, R., Ali Qarni, A., Haq, Z-U. & Amin, S. 2022. Synthesis and characterization of 2D MXene: Device fabrication for humidity sensing. *Journal of Science: Advanced Materials and Devices* 7(1): 100390.

Hu, Y., Xu, Z., Pu, J., Hu, L., Zi, Y., Wang, M., Feng, X. & Huang, W. 2022. 2D MXene $Ti_3C_2T_x$ nanosheets in the development of a mechanically enhanced and efficient antibacterial dental resin composite. *Frontiers in Chemistry* 10: 1090905.

Ikemoto, Y., Harada, Y., Tanaka, M., Nishimura, S-n., Murakami, D., Kurahashi, N., Moriwaki, T., Yamazoe, K., Washizu, H., Ishii, Y. & Torii, H. 2022. Infrared spectra and hydrogen-bond configurations of water molecules at the interface of water-insoluble polymers under humidified conditions. *The Journal of Physical Chemistry B* 126(22): 4143-4151.

Iqbal, A., Kwon, J., Kim, M-K. & Koo, C.M. 2021. MXenes for electromagnetic interference shielding: Experimental and theoretical perspectives. *Materials Today Advances* 9: 100124.

Islam, M.Z., Fu, Y., Deb, H., Hasan, M.K., Dong, Y. & Shi, S. 2023. Polymer-based low dielectric constant and loss materials for high-speed communication network: Dielectric constants and challenges. *European Polymer Journal* 200: 112543.

James, J.P. & Choi, S. 2024. Securing signal integrity: Innovative approaches to EMI reduction in converter systems. *Paper presented at the 2024 7th International Conference on Circuit Power and Computing Technologies (ICCPCT)*.

Jia, Z., Wang, C., Feng, A., Shi, P., Zhang, C., Liu, X., Wang, K. & Wu, G. 2020. A low-dielectric decoration strategy to achieve absorption dominated electromagnetic shielding material. *Composites Part B: Engineering* 183: 107690.

Karahan, B., Ozdemir, I., Grund, T., Hanisch, N. & Lampke, T. 2025. Advancements in cold spraying for polymer matrix composites: Enhanced LSP and EMI shielding performance - review and future directions. *Journal of Materials Science: Materials in Engineering* 20: 13.

Khalid, Z., Hadi, F., Xie, J., Chandrabose, V. & Oh, J-M. 2025. The future of MXenes: Exploring oxidative degradation pathways and coping with surface/edge passivation approach. *Small* 21(6): 2407856.

Kim, S. & Byun, J. 2024. Research trends in electromagnetic shielding using MXene-based composite materials. *Journal of Powder Materials* 31(1): 57-76.

Kumari, S., Dalal, J., Kumar, V., Kumar, A. & Ohlan, A. 2023. Emerging two-dimensional materials for electromagnetic interference shielding application. *International Journal of Molecular Sciences* 24(15): 12267.

Li, Y., Kankala, R.K., Chen, A-Z. & Wang, S-B. 2022. 3D printing of ultrathin MXene toward tough and thermally resistant nanocomposites. *Nanomaterials* 12(16): 2862.

Li, Z., Wang, L., Sun, D., Zhang, Y., Liu, B., Hu, Q. & Zhou, A. 2015. Synthesis and thermal stability of two-dimensional carbide MXene Ti_3C_2. *Materials Science and Engineering: B* 191: 33-40.

Ling, M., Ge, F., Wu, F., Zhang, L., Zhang, Q. & Zhang, B. 2024. Effect of crystal transformation on the intrinsic defects and the microwave absorption performance of Mo_2TiC_2Tx/RGO microspheres. *Small* 20(9): 2306233.

Lipatov, A., Alhabeb, M., Lukatskaya, M.R., Boson, A., Gogotsi, Y. & Sinitskii, A. 2016. Effect of synthesis on quality, electronic properties and environmental stability of individual monolayer Ti_3C_2 MXene flakes. *Advanced Electronic Materials* 2(12): 1600255.

Liu, W., Cao, J., Song, F., Zhang, D-D., Okhawilai, M., Yi, J, Qin, J-Q. & Zhang, X-Y. 2023. A double transition metal Ti2NbC2T_x MXene for enhanced lithium-ion storage. *Rare Metals* 42(1): 100-110.

Mendes, R.G., Ta, H.Q., Yang, X., Li, W., Bachmatiuk, A., Choi, J-H., Gemming, T., Anasori, B., Lijun, L., Fu, L., Liu, Z. & Rümmeli, M.H. 2020. *In situ* N-doped graphene and Mo nanoribbon formation from $Mo_2Ti_2C_3$ MXene monolayers. *Small* 16(5): 1907115.

Munir, S., Rasheed, A., Rasheed, T., Ayman, I., Ajmal, S., Rehman, A., Shakir, I., Agboola, P.O. & Warsi, M.F. 2020. Exploring the influence of critical parameters for the effective synthesis of high-quality 2D MXene. *ACS Omega* 5(41): 26845-26854.

Nasrin, K., Sudharshan, V., Subramani, K. & Sathish, M. 2022. Insights into 2D/2D MXene heterostructures for improved synergy in structure toward next-generation supercapacitors: A review. *Advanced Functional Materials* 32(18): 2110267.

Nguyen, Q-D. & Choi, C-G. 2024. Recent advances in multifunctional electromagnetic interference shielding materials. *Heliyon* 10(10): e31118.

Opara, F.A., Obasi, H.C., Eke, B.C. & Eze, W.U. 2023. Progress in polymer-based composites as efficient materials for electromagnetic interference shielding applications: A review. *Current Materials Science: Formerly: Recent Patents on Materials Science* 16(3): 235-261.

Osman, A., Elhakeem, A., Kaytbay, S. & Ahmed, A. 2022. A comprehensive review on the thermal, electrical, and mechanical properties of graphene-based multi-functional epoxy composites. *Advanced Composites and Hybrid Materials* 5(2): 547-605.

Park, J., Lee, W. & Kim, J. 2024. Large-scale construction and analysis of amorphous porous polymer network materials. *ACS Applied Materials & Interfaces* 16(42): 57190-57199.

Parker, T., Zhang, D., Bugallo, D., Shevchuk, K., Downes, M., Valurouthu, G., Inman, A., Chacon, B., Zhang, T., Shuck, C.E., Hu, Y-J. & Gogotsi, Y. 2024. Fourier-transform infrared spectral library of MXenes. *Chemistry of Materials* 36(17): 8437-8446.

Peng, M. & Qin, F. 2021. Clarification of basic concepts for electromagnetic interference shielding effectiveness. *Journal of Applied Physics* 130(22): 225108.

Protyai, M.I.H. & Rashid, A.B. 2024. A comprehensive overview of recent progress in MXene-based polymer composites: Their fabrication processes, advanced applications, and prospects. *Heliyon* 10(17): e37030.

Raagulan, K., Kim, B.M. & Chai, K.Y. 2020. Recent advancement of electromagnetic interference (EMI) shielding of two dimensional (2D) MXene and graphene aerogel composites. *Nanomaterials* 10(4): 702.

Ramesh, M., Rajeshkumar, L.N., Srinivasan, N., Kumar, D.V. & Balaji, D. 2022. Influence of filler material on properties of fiber-reinforced polymer composites: A review. *e-Polymers* 22(1): 898-916.

Tanvir, A., Sobolčiak, P., Popelka, A., Mrlik, M., Spitalsky, Z., Micusik, M., Prokes, J. & Krupa, I. 2019. Electrically conductive, transparent polymeric nanocomposites modified by 2D $Ti_3C_2T_x$ (MXene). *Polymers* 11(8): 1272.

Tu, S., Qiu, L., Liu, C., Zeng, F., Yuan, Y-Y., Hedhili, M.N., Musteata, V., Ma, Y., Liang, K., Jiang, N., Alshareef, H.N. & Zhang, X. 2024. Suppressing dielectric loss in MXene/polymer nanocomposites through interfacial interactions. *ACS Nano* 18(14): 10196-10205.

Ulas, B., Cetin, T., Topuz, M. & Akinay, Y. 2024. Ti_2NTx MXene materials derived from Ti_2AlN MAX phases: Their characterization and electrocatalytic activity toward hydrazine electrooxidation. *International Journal of Hydrogen Energy* 82: 892-900.

Umadevi, V. & Ranganathan, S. 2024. Evaluating the impact of radiated emissions from wireless devices on EMC in healthcare facilities. Paper presented at the 2024 *15th International Conference on Computing Communication and Networking Technologies (ICCCNT)*.

Verma, S., Dwivedi, U., Chaturvedi, K., Kumari, N., Dhangar, M., Hashmi, S.A.R., Singhal, R. & Srivastava, A.K. 2022. Progress of 2D MXenes based composites for efficient electromagnetic interference shielding applications: A review. *Synthetic Metals* 287: 117095.

Wong, A.J.Y., Lim, K.R.G. & Seh, Z.W. 2022. Fluoride-free synthesis and long-term stabilization of MXenes. *Journal of Materials Research* 37(22): 3988-3997.

Yang, Q., Gao, Y., Li, T., Ma, L., Qi, Q., Yang, T. & Meng, F. 2024. Advances in carbon fiber-based electromagnetic shielding materials: Composition, structure, and application. *Carbon* 226: 119203.

Zhang, J., Zhang, J., Shuai, X., Zhao, R., Guo, T., Li, K., Wang, D., Ma, C., Li, J. & Du, J. 2021. Design and synthesis strategies: 2D materials for electromagnetic shielding/absorbing. *Chemistry – An Asian Journal* 16(23): 3817-3832.

Zhang, Q., Wang, Q., Cui, J., Zhao, S., Zhang, G., Gao, A. & Yan, Y. 2023. Structural design and preparation of $Ti_3C_2T_x$ MXene/polymer composites for absorption-dominated electromagnetic interference shielding. *Nanoscale Advances* 5(14): 3549-3574.

*Corresponding author; email: fahmir@uthm.edu.my